I&EC research
Industrial & Engineering Chemistry Research

Article

Cite This: Ind. Eng. Chem. Res. 2018, 57, 3963−3976

pubs.acs.org/IECR

Simultaneous Process Scheduling and Control: A Multiparametric Programming-Based Approach

Baris Burnak,[†,‡] Justin Katz,[†,‡] Nikolaos A. Diangelakis,[†,‡] and Efstratios N. Pistikopoulos*[,†,‡]

[†]Artie McFerrin Department of Chemical Engineering, Texas A&M University, College Station, Texas 77845, United States
[‡]Texas A&M Energy Institute, Texas A&M University, College Station, Texas 77845, United States

Supporting Information

ABSTRACT: We present a systematic framework to derive model-based simultaneous strategies for the integration of scheduling and control via multiparametric programming. We develop offline maps of optimal scheduling actions accounting for the closed-loop dynamics of the process through a surrogate model formulation that incorporates the inherent behavior of the control scheme. The surrogate model is designed to translate the long-term scheduling decisions to time varying set points and operating modes in the time scale of the controller. The continuous and binary scheduling decisions are explicitly taken into account in the multiparametric model predictive controllers. We showcase the framework on a stand-alone three-product continuous stirred tank reactor, and two reactors operating in parallel.

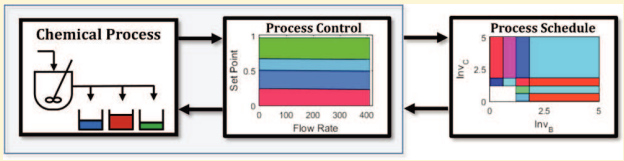

Downloaded via TEXAS A&M UNIV COLG STATION on July 9, 2018 at 20:22:04 (UTC).
See https://pubs.acs.org/sharingguidelines for options on how to legitimately share published articles.

1. INTRODUCTION

The traditional approach to assess the multiscale operational activities sequentially often leads to suboptimal solutions as each problem dictates different, and sometimes conflicting, objectives. The most recent advances in the field of operational research and the rapid reduction in the cost of computer hardware have enabled the integration of multiscale decision making mechanisms.[1−3] Production scheduling and process control are two layers in the process operations that are highly dependent due to the volume of reciprocal information flow. Typically, the process schedule coordinates the production sequence, production times, and inventory levels based on the market dynamics. Process control, on the other hand, delivers the production targets with the existence of operational uncertainty, measured/unmeasured process disturbances, and plant−model mismatch. These layers are typically addressed independently and sequentially due to the hierarchical nature of the underlying problems. The isolation between the decisions from different layers can result in suboptimal, or even infeasible operations.[4,5]

Individual assessment of the scheduling and control problems requires some assumptions that neglect the dynamics introduced by their complements. The scheduling problem utilizes static tables comprising the process time constants for the transitions between the operating modes of the system. These time constants are typically obtained by exhaustive closed-loop simulations conducted offline. Consequently, the static tables fail to represent the closed-loop dynamics of the system due to the lack of an underlying high-fidelity model.[6,7]

A simultaneous approach for process scheduling and control reconstructs the two problems as a unified problem. The reformulated problem takes into account the degrees of freedom of the two subproblems simultaneously, leading to an augmented feasible space. This allows the chemical plant to respond to rapidly changing market conditions while maintaining feasible and profitable operation. These changes include but are not limited to the market demand, price, and the spectrum and specifications regarding the products manufactured in the chemical plant. Furthermore, fluctuating operating costs require flexibility in the process scheduling.[8] Therefore, a chemical process needs integrated decisions that enable higher adaptability and operability to remain competitive in the market.[8] There have been some attempts over the years to tackle the two aspects of operational optimization in an integrated framework. An indicative list of these contributions is presented in Table 1.

Over two decades of academic literature on integrated approaches for the process scheduling and control problem has focused on a systematic methodology to overcome the following fundamental challenges:[47]

(i) Discrepancies in objectives: The schedule and control formulations are designed to deliver specialized tasks in a process. The former aims to bring profitable operation by taking into account the operational aspects such as the process economics, raw material, and equipment availability, and product specifications; while the latter involves real-time manipulation of select process variables to meet the targeted product specifications. These scheduling and control goals are not always aligned and frequently require the compromise of one of their respective objectives.

Received: October 26, 2017
Revised: February 22, 2018
Accepted: February 25, 2018
Published: February 26, 2018

© 2018 American Chemical Society

DOI: 10.1021/acs.iecr.7b04457
Ind. Eng. Chem. Res. 2018, 57, 3963−3976

Table 1. Scheduling and Control in the Literature: An Indicative List

author (year)	contribution
Grossmann and co-workers (2006a, 2006b, 2007, 2010, 2011, 2012, 2014),[7,9−14] Gudi and co-workers (2010),[15] Biegler and co-workers (2012, 2015),[16,17] You and co-workers (2013)[18]	simultaneous/decomposition (MI)DO or (MI)NLP and open-loop optimal control
Pistikopoulos and co-workers (2003a, 2003b),[19,20] You and co-workers (2012)[21]	simultaneous/decomposition (MI)DO schedule and P−PI−PID control
Allcock and co-workers (2002),[22] Espuña and co-workers (2013),[23] Baldea and co-workers (2014, 2015)[6,24]	simultaneous/decomposition algorithms using control/dynamics aware scheduling models
Biegler and co-workers (1996),[25] Barton and co-workers (1999),[26] Nyström and co-workers (2005),[27] Marquardt and co-workers (2008),[28] Ierapetritou and co-workers (2012),[29] You and co-workers (2013)[18]	simultaneous/decomposition algorithms via (MI)DO reformulation to (MI)NLP
Puigjaner and co-workers (1995),[30] Pistikopoulos and co-workers (2013, 2014, 2016),[3,31,32] Rawlings and co-workers (2012, 2013)[33,34]	control theory in scheduling problems
Marquardt and co-workers (2011),[35] Pistikopoulos and co-workers (2016, 2017, 2017),[3,36,37] Ierapetritou and co-workers (2016)[38]	advanced control and (MI)NLP scheduling schemes
Reklaitis and co-workers (1999),[39] Floudas and co-workers (2004, 2007),[40,41] Ricardez-Sandoval and co-workers (2015, 2017),[42,43] You and co-workers (2015)[44]	scheduling under uncertainty
Reklaitis and co-workers (1996),[45] Floudas and co-workers (2004),[46] Grossmann (2005),[1] Nyström and co-workers (2009),[8] Engell and Harjunkoski (2012),[4] Baldea and co-workers (2014),[5] You and co-workers (2015),[44] Ierapetritou and co-workers (2016)[38]	review articles on scheduling and control and metholodogies

(ii) Discrepancies in time-scales: A typical control horizon varies between seconds and minutes, whereas the scheduling horizon is on the order of hours or weeks. Therefore, integration of the two distinct problems into a unified formulation creates a large scale, stiff system due to the order of magnitude differences in their respective time scales.[6,47] Following direct solution approaches for the reformulated unified problem has been shown to be computationally intractable.[17]

In this study, we propose a surrogate model formulation that bridges the inherent gap between the schedule and control formulations. The surrogate model is designed to translate the fast closed-loop dynamics to the slower scheduling dynamics, while providing corrective time varying targets for the controller. We utilize the reactive scheduling approach introduced by Subramanian et al.,[33] and adapted in a multiparametric framework by Kopanos and Pistikopoulos,[32] formulating a state-space representation that is implemented in a rolling horizon framework. This formulation is solved once and offline via multiparametric programming techniques, deriving optimal scheduling decisions as affine functions of the product demand scenarios. The derivation of the controllers, on the other hand, is adapted from the PARametric Optimization and Control (PAROC) framework,[48] which provides a systematic methodology to design advanced model-based controllers via multiparametric programming. The framework is tailored to account for the scheduling decisions explicitly.

The remainder of the paper is organized as follows. The proposed methodology to derive an integrated process schedule and control is described in section 2 in detail and showcased on a three product CSTR, and two CSTRs in parallel in section 3. The concluding remarks on the application of the framework and the future directions to extend its implementation is provided in section 4.

2. INTEGRATION OF CONTROL AND SCHEDULING VIA PAROC

2.1. Problem Definition. The following generalized problem definition presents the long-term (schedule) and short-term (control) objectives simultaneously.

(i) Given: a dynamic model of the system of interest, process constraints regarding the safety issues and product specifications, unit cost for inventory, a scenario of the market conditions.
(ii) Determine: production sequence, target production rate, optimal control actions to achieve the target production rate.
(iii) Objective: minimize the total cost comprising the inventory, transition, and raw material costs.

We propose a systematic framework that features the following:

- a single high fidelity model based on which we seek to derive an integrated scheduling and control scheme
- a scheduling scheme, aware of the short-term dynamics
- a control scheme, aware of the longer term scheduling/operational decisions
- an offline map of optimal short-term and long-term operational actions

2.2. Problem Formulation. The problem defined in section 2.1 is represented with a generalized mathematical model in the form of a MIDO problem.[49]

$$\begin{aligned}
\min_{u,S,Y} \quad & J = \int_0^\tau P(x, y, u, S, Y, d)\, \mathrm{d}t \\
\text{s.t.} \quad & \frac{\mathrm{d}}{\mathrm{d}t}x = f(x, u, S, Y, d) \\
& y_{\min} \le y = g(x, u, S, Y, d) \le y_{\max} \\
& u_{\min} \le u = h(x, y, S, Y, d) \le u_{\max} \\
& S_{\min} \le S = m(x, y, Y, d) \le S_{\max} \\
& Y \in \{0, 1\} \\
& [x_{\min}^T, d_{\min}^T]^T \le [x^T, d^T]^T \le [x_{\max}^T, d_{\max}^T]^T
\end{aligned} \tag{1}$$

where x stands for the states of the system, y is the system outputs, u is the optimal control actions, S and Y are the continuous and binary scheduling decisions respectively, d is the measured disturbances to the system and the market conditions, P is the objective function of the system accounting for the short-term and long-term operational costs, f and g are the first principle system equations, and h and m are the

DOI: 10.1021/acs.iecr.7b04457
Ind. Eng. Chem. Res. 2018, 57, 3963−3976

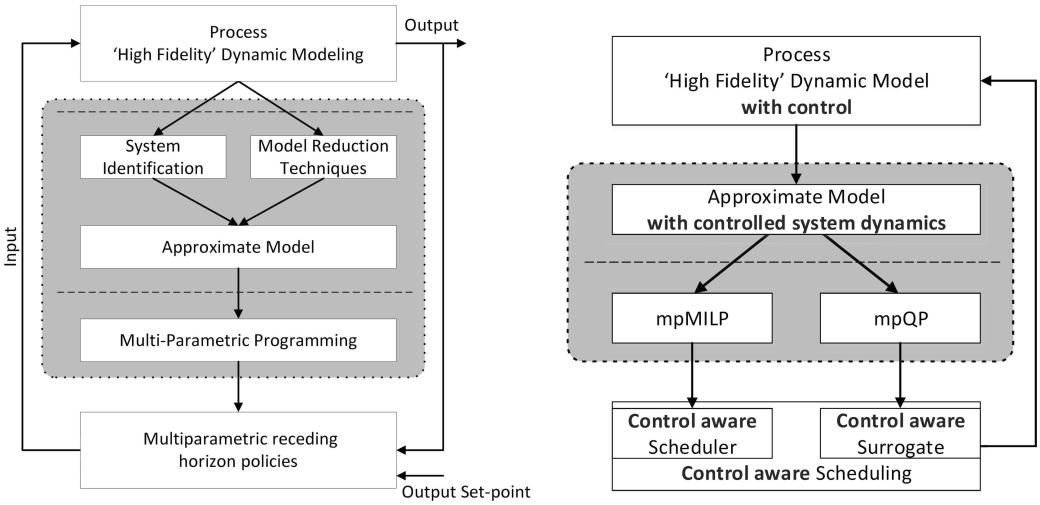

(a) Derivation of the control scheme (b) Derivation of the scheduling scheme

Figure 1. (a) The steps of the PAROC framework;[48] (b) proposed methodology to derive integrated schedule and control (adapted from ref 36). Actions within the gray area happen once and offline.

optimal control and scheduling actions. On the basis of the problem definition stated in section 2.1, (i) we are given the process model f and g, operational cost function P, a scenario of the market conditions $d^s \subseteq d$, and operational upper $(\cdot)_{max}$ and lower $(\cdot)_{min}$ bounds, and (ii) we aim to determine the production sequence Y, target production rate S, and control actions u (iii) that minimize the operational costs over a time horizon.

Equation 1 typically describes a nonlinear and nonconvex problem that requires simplifying assumptions or advanced decomposition techniques. The fundamental complexity of this class of problems stems from (i) the computational cost of the integration of short-term regulatory control decisions with relatively longer time horizons, and (ii) incorporating economic considerations in short-term decisions.[6]

In this work, we propose the use of the PAROC framework[48] to decompose the overall problem into two main steps. The proposed methodology consists of (i) acquiring scheduling dependent explicit control schemes and (ii) developing long-term scheduling strategies based on the high fidelity process model featuring the control scheme derived in the first step.

2.3. The PAROC Framework and Software Platform. The PAROC framework provides a comprehensive environment to design chemical processes, to build controllers, and to perform parameter estimation based on high-fidelity models benefiting from the most recent advances in the field of multiparametric programming.[48] In our previous work[50] we have presented the applicability of this framework on the integration of process design and control. In this study, we provide a generic methodology to apply PAROC to carry out short-term and long-term operational optimization simultaneously.

The first step of the proposed method is to acquire a mathematical model "high-fidelity" to describe the system of interest with sufficient accuracy. These models are typically very large in size and/or complex in nature, rendering it difficult to apply an advanced optimization algorithm. Therefore, the original mathematical model is approximated or reduced in size via the existing algorithms in the literature. Note that the approximate model features the scheduling aspects of the system as additional dimensions in order to generate a schedule-aware control scheme. A model predictive control (MPC) scheme is constructed using the approximate model, and solved multiparametrically (mpMPC) to generate offline maps of optimal control actions. These maps are embedded into the original mathematical model, and a control-aware approximate model is derived to describe the closed-loop behavior of the system. The resulting model is used to derive offline maps of (i) long-term decisions regarding the operational feasibility and profitability and (ii) a surrogate model to bridge the gap between the short-term and long-term decisions. The offline maps are validated against the "high-fidelity" model used in the first step. A schematic representation of the proposed methodology is presented in Figure 1. The closed-loop implementation of the framework and the fundamental interactions between different layers of models for the integration of schedule and control are depicted in Figure 2.

Note the following advantages of solving the multiparametric counterparts of the schedule, control, and time scale bridging surrogate model:

- Offline maps of optimal operations at both long and short terms are acquired as explicit expressions.

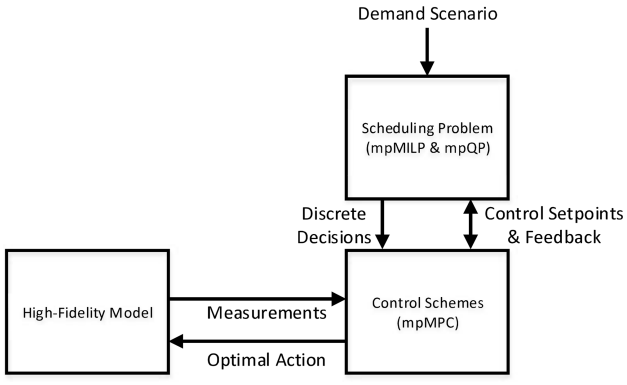

Figure 2. Schematic representation of the simultaneous scheduling and control (adapted from ref 36).

DOI: 10.1021/acs.iecr.7b04457
Ind. Eng. Chem. Res. 2018, 57, 3963−3976

- Online computational time for the optimal control problem is reduced to a simple look-up table algorithm and evaluation of an affine function. Such significant reduction enables the application of the framework to systems with fast dynamics.
- The offline maps of solutions can allow for the integration of the design of the process/equipment with the schedule and control in a dynamic optimization framework.

Following are the fundamental steps of PAROC in further detail, tailored specific to the needs of the simultaneous scheduling and control problem.

Designing Schedule-Aware Controller. Step 1: "High-fidelity" dynamic modeling. A rigorous and robust model based on first-principles, typically differential algebraic equations (DAEs) or partial differential algebraic equations (PDAEs), is used to simulate the dynamics of the system. In this work, we use the gPROMS environment to construct the model, as described with a general representation in eq 2.

$$\frac{\mathrm{d}}{\mathrm{d}t}x(t) = f(x(t), u(t), S(t), Y(t), d(t), t)$$
$$y(t) = g(x(t), u(t), S(t), Y(t), d(t), t) \tag{2}$$

where $S(t)$ is a generic expression that encompasses the set points on the outputs, $y^{SP}(t)$, set points on the inputs, $u^{SP}(t)$, and the degrees of freedom of the system that is determined by the scheduler and unavailable to the controller $Sc(t)$.

Step 2: Model approximation: The high-fidelity model designed in Step 1 usually comprises highly nonlinear and nonconvex terms that render the practice of advanced control algorithms quite challenging. Therefore, we appeal to system identification or model reduction techniques to approximate the model formulation with a discrete time affine state space representation. In this work, the model approximation is performed via the MATLAB System Identification Toolbox yielding the state space representation in eq 3. Note that the system identification techniques may or may not preserve the physical meanings of the original states in eq 2.

$$x^q_{t_c+1} = A^q\cdot x^q_{t_c} + B^q\cdot u_{t_c} + C^q\cdot[d^T_{t_c}, \mathrm{Sc}^T_{t_c}]^T$$
$$\hat{y}_{t_c} = D^q\cdot x^q_{t_c} + E^q\cdot u_{t_c} + F^q\cdot[d^T_{t_c}, \mathrm{Sc}^T_{t_c}]^T \tag{3}$$

where index t_c indicates the discrete time steps sampled in control scale, superscript q denotes the index of the linear model, and $\hat{y}$ is the output predicted by the approximate model. Note that the states $x^q_{t_c}$ can be concatenated into a single vector, x_{t_c}.

Equation 3 is a generalized reduced expression that represents the dynamics between the manipulated inputs, measured disturbances, and outputs of the system. Note that the reduced model also features the degrees of freedom of the system that may be fixed by the scheduler and unavailable to the controller, Sc_{t_c}.

The validity of the approximate model is essential for the closed loop performance of the system. The approximate model is considered acceptable if (i) it yields a good fit against an input−output test set, (ii) the cross-correlation between the inputs and the residual outputs is within the confidence intervals, (iii) it is open loop stable within the range of inputs, and (iv) no single pole is canceled by a zero to satisfy the necessary and sufficient condition of controllability. In the case of an inadequate representation of the high fidelity model, the number of piecewise models can be incremented at the expense of increasing the computational time to derive the control strategies in the next step.

Step 3: Design of the multiparametric model predictive controller (mpMPC). The state space model given in eq 3 is used to build a mpMPC following the procedure described in our previous work.[48,50,51] Note that the mpMPC is aware of the scheduling level decisions since the state space model incorporates them as measured disturbances. Equation 4 describes the general form of the mpMPC formulation used in this work.

$$\begin{aligned}
\min_{u_{t_c}}\quad & J(\theta) = x^T_{N_c}Px_{N_c} + \sum_{t_c=1}^{N_c-1} x^T_{t_c}Q_{t_c}x_{t_c} \\
& + \sum_{t_c=1}^{N_c-1}(y_{t_c} - y^{SP}_{t_c})^T QR_{t_c}(y_{t_c} - y^{SP}_{t_c}) \\
& + \sum_{t_c=0}^{M_c-1}(u_{t_c} - u^{SP}_{t_c})^T R_{t_c}(u_{t_c} - u^{SP}_{t_c}) \\
& + \sum_{t_c=0}^{M_c-1}\Delta u^T_{t_c}R1_{t_c}\Delta u_{t_c} \\
\text{s.t.}\quad & x_{t_c+1} = A\cdot x_{t_c} + B\cdot u_{t_c} + C\cdot[d^T_{t_c}, \mathrm{Sc}^T_{t_c}]^T \\
& \hat{y}_{t_c} = D\cdot x_{t_c} + E\cdot u_{t_c} + F\cdot[d^T_{t_c}, \mathrm{Sc}^T_{t_c}]^T \\
& y_{t_c} = \hat{y}_{t_c} + e \\
& e = y_{t_c=0} - \hat{y}_{t_c=0} \\
& \theta = [x^T_{t_c=0}, u^T_{t_c=-1}, d^T_{t_c=0}, \mathrm{Sc}^T_{t_c}, (y^{SP}_{t_c})^T, (u^{SP}_{t_c})^T, Y^T_{t_c}, y^T_{t_c=0}]^T \\
& x_{\min,t_c} \le x_{t_c} \le x_{\max,t_c} \\
& y_{\min,t_c} \le y_{t_c} \le y_{\max,t_c} \\
& u_{\min,t_c} \le u_{t_c} \le u_{\max,t_c} \\
& \Delta u_{\min,t_c} \le \Delta u_{t_c} \le \Delta u_{\max,t_c} \\
& \forall\, t_c \in \{0, 1, ..., N_c - 1\}
\end{aligned} \tag{4}$$

where x_{t_c} is the state variables, y_{t_c} is the system outputs, u_{t_c} is the control variables, Δu_{t_c} is the magnitude between two consecutive control actions, d_{t_c} is measured disturbances, Q_{t_c}, QR_{t_c}, R_{t_c}, $R1_{t_c}$ are the corresponding weights in the objective function, P is the stabilizing term determined by solving the discrete time algebraic Ricatti equation, N_c and M_c are the output horizon and control horizon, respectively. e denotes the plant-model mismatch and is defined as the difference between the real output measured and the state space estimation of the output at $t_c = 0$. $y^{SP}_{t_c}$ and $u^{SP}_{t_c}$ are the output set points and input reference points, respectively. Note that these two vectors of variables are scheduling level decisions (i.e., $\{y^{SP}_{t_c}, u^{SP}_{t_c}\} \subseteq S$), and hence mpMPC treats them as additional parameters in θ.

The minimization problem presented in eq 4 is translated into a linearly constrained quadratic multiparametric program-

DOI: 10.1021/acs.iecr.7b04457
Ind. Eng. Chem. Res. 2018, 57, 3963−3976

ming problem (mpQP) via the YALMIP toolbox,[52] and solved via the Parametric OPtimization (POP) Toolbox[53] in MATLAB. The solution of the mpQP problem yields explicit control actions as an affine function of the uncertain parameters, as presented in eq 5.

$$
\begin{aligned}
&u_j(\theta) = K_n\theta + r_n,\ \forall\ \theta \in CR_n\\
&\theta := [x_{t_c=0}^T,\ u_{t_c=-1}^T,\ d_{t_c=0}^T,\ \mathrm{Sc}_{t_c}^T,\ (y_{t_c}^{SP})^T,\ (u_{t_c}^{SP})^T,\ Y_{t_c}^T,\ y_{t_c=0}^T]^T\\
&CR_n := \{\theta \in \Theta \mid L_n\theta \le b_n\},\ \forall\ n \in \{1, 2, \ldots NC\}\\
&\forall\ j \in \{0, 1, \ldots, M_c\},\ \forall\ t_c \in \{0, 1, \ldots, N_c\}
\end{aligned}
\tag{5}
$$

where θ is the set of uncertain parameters measured at $t_c = 0$, $u_{t_{c-1}}$ is the optimal control action at the previous time step, CR_n is the active polyhedral partition of the feasible parameter space, NC is the number of critical regions CR_n, and Θ are defined as a closed and a bounded set. Note that inclusion of scheduling level decisions, that is, $y_{t_c}^{SP}$, $u_{t_c}^{SP}$, and Y_{t_c} in the parameter space enables mpMPC to account for any future changes in the operational level a priori within the range of the output horizon.

Step 4: Closed-loop validation. Since the framework suggests an approximation of the high fidelity model, a validation step is mandatory to test the validity of the simplified model, as well as the controller scheme. Therefore, the mpMPC derived in Step 3 is validated through in-silico testing against the high fidelity model in Step 1. The assessment of the closed loop performance, including but not limited to efficient set point tracking, fast adaptation to changes in the operational level, constraint violation, and operational stability dictates whether a new approximate model is required or we can proceed to the next step to design the scheduler.

gPROMS provides interconnectivity with MATLAB via (i) a gO:MATLAB object to enable working in the MATLAB environment, or (ii) C++ programming and creation of Dynamic Link Libraries (.dll) for straight implementation of the controllers in gPROMS environment. Hence, closed-loop simulations can be conducted using either software.

Designing Control-Aware Scheduler. Production scheduling of a chemical process formulated as a general MILP problem can also be represented by a state space model.[33,34] A multiparametric counterpart of this class of reactive scheduling problems and its solution is described extensively in Kopanos and Pistikopoulos.[32] This approach yields an optimal map of solutions under potential disruptions in the course of operation prior to the occurrence of the event. The explicit form of the schedule significantly reduces the computational cost of repetitive evaluations after every disruptive event. However, the sampling time of the state space model is typically too large to account for the dynamic considerations inherent to the process. Hence, such an approach suggests utilization of static transition tables based on exhaustive testing[6] that create plant-model mismatch since they are agnostic to the real system dynamics.

In this work, we propose a two level scheduling scheme with a hierarchical order: (i) upper level schedule for the regulation of the economic considerations and operational feasibility based on the formulation of Kopanos and Pistikopoulos,[32] and (ii) lower level surrogate model to bridge the time scales between the control and the upper level schedule based on the closed loop behavior of the high fidelity model. The surrogate model further aims to remedy the plant-model mismatch introduced by the schedule.

Step 1: "High-fidelity" model with controller embedded. The control scheme derived in the earlier phase (eq 5) is embedded in the original high fidelity model (eq 2).

Step 2: Approximate models. A discrete time state space model is derived based on the closed loop behavior of the high fidelity model. The input−output relationship focuses on capturing the overall response of the closed loop system to the step changes in the output set points and input reference points. Note that the discretization time of the identified model for the upper level scheduler is several orders of magnitude larger than the mpMPC. Therefore, we introduce a surrogate model formulation to translate the upper level scheduling decisions in the first scheduling time step into the control time steps. This translation is carried out by resampling the identified scheduling model with a discretization step matching the output horizon of the mpMPC. The resampled model is used as the governing constraint in the surrogate model formulation, as described in detail in the next step.

Step 3: Design of the multiparametric schedule and surrogate model. The multiparametric schedule is formulated with an objective to account for the economic considerations and operational feasibility, subjected to the corresponding approximate model derived earlier, as described in Kopanos and Pistikopoulos.[32] The resulting formulation creates a mpMILP that treats the disruptive scheduling events as parameters described in eq 6.

$$
\begin{aligned}
\min_{\tilde{u}_{t_s}, Y_{t_s}}\ & J(\theta) = \sum_{t_s=1}^{N_s} \alpha^T \tilde{x}_{t_s} + \sum_{t_s=0}^{N_s-1} \beta^T \widetilde{tr}_{t_s} + \sum_{t_s=0}^{N_s} \phi^T \tilde{u}_{t_s}\\
\text{s.t.}\ & \tilde{x}_{t_s+1} = A_1\tilde{x}_{t_s} + B_1\tilde{u}_{t_s} + C_1\tilde{d}_{t_s}\\
& \widetilde{tr}_{t_s} = A_2(\tilde{x}_{t_s} - \tilde{x}_{t_s-1}) + B_2(\tilde{u}_{t_s} - \tilde{u}_{t_s-1})\\
& \tilde{u}_{t_s} = [\widetilde{Sc}_{t_s}^T,\ (\tilde{y}_{t_s}^{SP})^T,\ (\tilde{u}_{t_s}^{SP})^T]^T\\
& \theta = [\tilde{x}_{t_s=0}^T,\ \tilde{x}_{t_s=-1}^T,\ \tilde{u}_{t_s=-1}^T,\ \tilde{d}_{t_s}^T]^T\\
& \tilde{x}_{\min,t_s} \le \tilde{x}_{t_s} \le \tilde{x}_{\max,t_s}\\
& \widetilde{tr}_{\min,t_s} \le \widetilde{tr}_{t_s} \le \widetilde{tr}_{\max,t_s}\\
& \tilde{u}_{\min,t_s}Y_{t_s} \le \tilde{u}_{t_s} \le \tilde{u}_{\max,t_s}Y_{t_s}\\
& \forall\ t_s \in \{0, 1, \ldots, N_s\}
\end{aligned}
\tag{6}
$$

where the tilde (∼) sign denotes a scheduling level counterpart of the variable, $\tilde{x}$ is the operational level and the inventory, $\widetilde{tr}$ denotes transition to a different operational mode, and the Greek letters α, β, and ϕ are the corresponding cost parameters. Note that additional constraints can be included in eq 6 regarding the needs of the specific problem. The linear state space matrices represent the closed loop dynamics of the system, and acquired through the MATLAB System Identification Toolbox or a model reduction technique, as described by Diangelakis.[54] The multiparametric solution of eq 6 provides explicit affine expressions of the optimal scheduling actions as functions of the system parameters, as defined in eq 7.

DOI: 10.1021/acs.iecr.7b04457
Ind. Eng. Chem. Res. 2018, 57, 3963−3976

$$[\tilde{u}_{t_s}^T(\theta),\ Y_{t_s}^T(\theta)]^T = \tilde{K}_n\theta + \tilde{r}_n,\ \forall\ \theta \in CR_n$$
$$\theta := [\tilde{x}_{t_s=0}^T,\ \tilde{x}_{t_s=-1}^T,\ \tilde{u}_{t_s=-1}^T,\ \tilde{d}_{t_s}^T]^T$$
$$CR_n := \{\theta \in \Theta \mid \tilde{L}_n\theta \le \tilde{b}_n\},\ \forall\ n \in \{1, 2, \ldots NC\}$$
$$\forall\ t_s \in \{0, 1, \ldots, N_s\} \tag{7}$$

Due to approximation of the scheduling model and the large discretization time, there exists a plant-model mismatch that is handled by a surrogate model formulated as a mp(MI)QP. Therefore, we utilize the formulation presented in eq 8 to minimize the aforementioned mismatch.

$$\min_{S_{t_{sm}}}\ J(\theta) = \sum_{t_{sm}=0}^{N_{sm}} (S_{t_{sm}} - \tilde{u}_{t_s})^T R' (S_{t_{sm}} - \tilde{u}_{t_s})$$
$$\text{s.t.}\quad x'_{t_{sm}+1} = Ax'_{t_{sm}} + BS_{t_{sm}}$$
$$y_{t_{sm}} = Cx'_{t_{sm}} + DS_{t_{sm}}$$
$$S_{t_{sm}} = [Sc_{t_{sm}}^T,\ (y_{t_{sm}}^{SP})^T,\ (u_{t_{sm}}^{SP})^T]^T$$
$$\theta = [\tilde{u}_{t_{sm}}^T,\ Y_{t_{sm}}^T]$$
$$x'_{\min,t_{sm}} \le x_{t_{sm}} \le x'_{\max,t_{sm}}$$
$$y_{\min,t_{sm}} \le y_{t_{sm}} \le y_{\max,t_{sm}}$$
$$S_{\min,t_{sm}}Y_{t_{sm}} \le S_{t_{sm}} \le S_{\max,t_{sm}}Y_{t_{sm}}$$
$$\forall\ t_{sm} \in \{0, 1, \ldots, N_{sm}\} \tag{8}$$

Equation 8 poses a mpQP problem that reinterprets the scheduling actions $\tilde{u}_{t_s}$ in the time steps of the controller. $Sc_{t_{sm}}$ is directly passed to the process, and the set points $y_{t_{sm}}^{SP}$ and $u_{t_{sm}}^{SP}$ are determined to be used by the controller. Δt_{sm} is based on the output horizon of the mpMPC ($\Delta t_{sm} = \Delta t_c N_c$), and N_{sm} is selected such that the surrogate model horizon can account for the first scheduling time step in its entirety (i.e., $N_{sm} \ge \Delta t_s/\Delta t_{sm}$). The multiparametric solution to eq 8 yields an offline map of optimal scheduling actions and set points for the controller, allowing for fast reevaluation of the scheduling decisions under varying market conditions. The surrogate model formulation utilizes a linear state space representation of the closed loop dynamics of the system. Therefore, the number of state space models required to capture the complete dynamics is dependent on the complexity of the high fidelity model and the size of the explicit control law. The validity of these surrogate models representations is assured in the subsequent step.

Note that binary decisions $Y_{t_{sm}}$ from eq 6 are treated as continuous uncertain parameters. Oberdieck et al.[55] presents a rigorous proof through the Basic Sensitivity Theorem that relaxation of the binary parameters yields the exact solution in this class of problems. Equivalently, one can generate 2^n mpQP problems to exhaustively enumerate all combinations of binary parameter realizations, where n is the number of binary parameters.

Step 4: Closed-loop validation. Overall validation of the integrated schedule-control scheme is performed in a rolling horizon fashion through utilization of the maps of solutions generated with eqs 4, 6, and 8 simultaneously on the high fidelity model (eq 2). The overall system is subjected to randomized market conditions that is updated in the time steps of the scheduler to yield the input and output trajectories in the scheduling and control levels. The interplay and the flow of information among the multiparametric scheduler, surrogate model, controller, and the process is summarized and depicted in Figure 3.

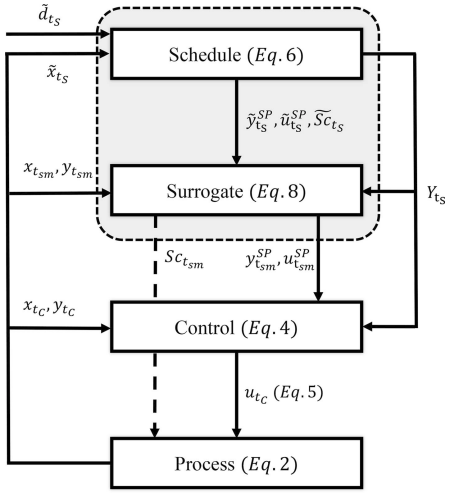

Figure 3. Information flow among the scheduler, surrogate model controller, and the process. The gray area indicates the overall control-aware scheduler.

Note that the framework assumes an update in the disruptive events at the time steps of the schedule. Any further scheduling level disturbances in between these time steps can be addressed by reevaluating the set points through the surrogate model to remedy a potential performance degradation. The process disturbances, on the other hand, are accounted for by the controller of which dynamics are embedded in the scheduler.

The following section presents the application of the framework on (i) a CSTR with three reactants and three outputs, and (ii) two CSTRs operated in parallel.

3. EXAMPLES

3.1. Example 1. Single CSTR with Three Inputs and Three Outputs. *Problem Definition.* This case study, adapted from Flores-Tlacuahuac and Grossmann,[7] considers an isothermal CSTR designed to manufacture three products on a single production line, as depicted in Figure 4. In the figure, R_i

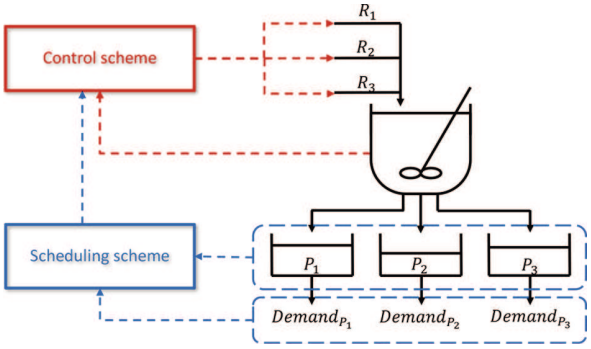

Figure 4. CSTR flowsheet with the online implementation of the scheduling and control schemes.

DOI: 10.1021/acs.iecr.7b04457
Ind. Eng. Chem. Res. 2018, 57, 3963−3976

denotes the ith reactant, P_j denotes the jth product, and $Demand_{P_j}$ denotes the demand rate for product P_j. The problem statement encompasses the following:

(i) Given: a high-fidelity model of the three product CSTR, unit cost for inventory, a scenario of product demands
(ii) Determine: production sequence, production rates, optimal control actions to achieve the target production rate and to reach the threshold purity
(iii) Objective: minimize the total cost comprising the inventory and transition costs

On the basis of the described problem definition, the control scheme aims to determine the optimal transitions between the production periods of three products through tracking a time variant product concentration set point to maintain a certain level of purity threshold. The controller is designed to deliver this short-term objective by manipulating the feed composition at the inlet of the reactor, and monitoring the states of the system. To obtain the longer term objectives, we utilize a scheduling scheme to minimize the operating and inventory costs, while satisfying a continuous demand rate for each product. The scheduler aims to determine the optimal production sequence and manufacturing time, while accounting for the inventory levels in the storage tanks and a demand scenario. The scheduling decisions are passed on to the controller as set points and operating modes.

Note that different from that of Flores-Tlacuahuac and Grossmann,[7] this work relaxes the assumption of constant product demand rate profile, and considers a variable demand rate profile.

High-Fidelity Dynamic Model. Three irreversible reactions take place in parallel in the CSTR reaction network given in eq 9.

$$\begin{aligned} 2R_1 &\xrightarrow{k_1} P_1 \\ R_1 + R_2 &\xrightarrow{k_2} P_2 \\ R_1 + R_3 &\xrightarrow{k_3} P_3 \end{aligned} \tag{9}$$

where k_1, k_2, and k_3 are the rate constants of the respective reactions. Note that production of P_1 requires only R_1, which also features as one of the raw materials of products P_2 and P_3. Hence, the given reaction network yields P_1 as a byproduct during the production phases of P_2 and P_3. The byproduct concentration degrades the purity of the product of interest, and needs to be accounted for by the control scheme to achieve high selectivity.

The high-fidelity model that describes the dynamic behavior of the CSTR comprises mole balances (eq 10) and power law kinetic expressions for elementary reactions (eq 11).

$$\begin{aligned} \frac{dC_{R_i}}{dt} &= \frac{Q_{R_i}C_{R_i}^f - Q_{\text{total}}C_{R_i}}{V} + \mathcal{R}_{R_i} \\ \frac{dC_{P_j}}{dt} &= \frac{Q_{\text{total}}(C_{P_j} - C_{P_j})}{V} + \mathcal{R}_{P_j} \end{aligned} \tag{10}$$

$$\begin{aligned} \mathcal{R}_{R_1} &= -2\mathcal{R}_{P_1} - \mathcal{R}_{P_2} - \mathcal{R}_{P_3} \\ \mathcal{R}_{R_2} &= -\mathcal{R}_{P_2} \\ \mathcal{R}_{R_3} &= -\mathcal{R}_{P_3} \\ \mathcal{R}_{P_1} &= k_1 C_{R_1}^2 \\ \mathcal{R}_{P_2} &= k_2 C_{R_1} C_{R_2} \\ \mathcal{R}_{P_3} &= k_3 C_{R_1} C_{R_3} \end{aligned} \tag{11}$$

where C denotes the concentration, Q is the volumetric flow rate, V is the volume of the CSTR, $\mathcal{R}$ is the reaction rate, superscript f denotes the feed to the CSTR, R_i and P_j are the indices for the ith reactant and jth product, respectively. The system parameters are given in Table 2.

Table 2. Parameters of the High-Fidelity CSTR Model

reaction rate constants	value	reactant concentration at the feed	value
k_1	0.1	$C_{R_1}^f$	1.0
k_2	0.9	$C_{R_2}^f$	0.8
k_3	1.5	$C_{R_3}^f$	1.0

The total volumetric flow rate is defined as the sum of reactant flow rates at the inlet of the reactor. Note that constant volume reactor is assumed, therefore the total flow rate at the inlet is equal to the total flow rate at the outlet.

$$Q_{\text{total}} = \sum_i Q_{R_i} \tag{12}$$

The inventory levels of the product of interest are as follows.

$$\frac{dW_{P_j}}{dt} = \begin{cases} Q_{\text{total}}C_{P_j} - DR_{P_j}, & \text{if } Pur_{P_j} \geq 0.90 \\ -DR_{P_j}, & \text{if } Pur_{P_j} < 0.90 \end{cases} \tag{13}$$

where W_{P_j} is the inventory level, DR_{P_j} is the demand rate, and Pur_{P_j} is the purity level in the CSTR as defined in eq 14.

$$Pur_{P_j} = \frac{C_{P_j}}{\sum_j C_{P_j}} \tag{14}$$

The molar fractions of the reactant flow rates are defined in eq 15. Note that the molar fractions are utilized as the manipulated variables in the mpMPC control scheme, as demonstrated in the following sections.

$$\begin{aligned} a_{R_i} &= \frac{Q_{R_i}}{Q_{\text{total}}} \\ \sum_i a_{R_i} &= 1 \end{aligned} \tag{15}$$

Model Approximation. The highly nonlinear nature of the model necessitates partitioning of the input space to capture the system dynamics with higher accuracy. Rigorous simulations of the high fidelity model suggest the partitioning of each degree of freedom available to the controller (i.e., a_{R_2} and a_{R_3}) to at least two mutually exclusive subspaces, respectively. Hence, the discrete time state space model generated in MATLAB System Identification Toolbox has the following form.

DOI: 10.1021/acs.iecr.7b04457
Ind. Eng. Chem. Res. 2018, 57, 3963−3976

$$x_{t_c+1} = A_c x_{t_c} + B_c u_{t_c} + C_c d_{t_c}$$
$$y_{t_c} = D_c x_{t_c} \tag{16}$$

$$u_{t_c} = [u_{1,t_c}, u_{2,t_c}, u_{3,t_c}, u_{4,t_c}]^T$$
$$u_{1,t_c} = a_{R_2},\ a_{R_2} \in [0, 0.5)$$
$$u_{2,t_c} = a_{R_2},\ a_{R_2} \in [0.5, 1]$$
$$u_{3,t_c} = a_{R_3},\ a_{R_3} \in [0, 0.55)$$
$$u_{4,t_c} = a_{R_3},\ a_{R_3} \in [0.55, 1] \tag{17}$$

where x_{t_c} is the identified states, u_{t_c} is the molar fractions of the reactant flow rates partitioned in the input space as given in eq 17, d_{t_c} is the total volumetric flow rate (Q_{total}), and y_{t_c} is the product concentrations (C_{P_j}). The state space matrices are given in the Supporting Information. Note that a_{R_1} is excluded from the manipulated variables due to the linear independence of the molar fractions.

The step and impulse responses of the open loop approximate model are stable within the range of inputs, as presented in Figures S1 and S2, respectively.

Design of the mpMPC. The formulation of the mpMPC is based on eq 4 with additional soft constraints included as presented in eq 18. The tuning of the corresponding parameters is based on heuristic MPC design methods, and the parameters are provided in Table 3.

$$\min_{u_{t_c}, z_{t_c}, \varepsilon_{t_c}} J(\theta) = \sum_{t_c=1}^{N_c} (y_{t_c} - y_{t_c}^{SP})^T QR (y_{t_c} - y_{t_c}^{SP}) + \sum_{t_c=0}^{M_c-1} \Delta u_{t_c}^T R1 \Delta u_{t_c} + \sum_{t_c=1}^{N_c} \varepsilon_{t_c}^T P1 \varepsilon_{t_c}$$

s.t.
$$x_{t_c+1} = A_c x_{t_c} + B_c u_{t_c} + C_c d_{t_c}$$
$$\hat{y}_{t_c} = D x_{t_c}$$
$$y_{t_c} = \hat{y}_{t_c} + e$$
$$e = y_{t_c=0} - \hat{y}_{t_c}$$
$$x_{\min} \le x_{t_c} \le x_{\max}$$
$$y_{\min} \le y_{t_c} \le y_{\max}$$
$$u_{\min} z_{t_c} \le u_{t_c} \le u_{\max} z_{t_c}$$
$$u_{\min} Y_{t_c} \le u_{t_c} \le u_{\max} Y_{t_c}$$
$$d_{\min} \le d_{t_c} \le d_{\max}$$
$$\Delta u_{\min} \le \Delta u_{t_c} \le \Delta u_{\max}$$
$$-y_{*,t_c} + Pur_{\min} \sum_i y_{i,t_c} \le -\varepsilon_{t_c} + \mathcal{M} Y_{t_c}$$
$$0 \le \varepsilon_{t_c} \le 1,\ z_{t_c} \in \{0, 1\}$$
$$\theta = [x_{t_c=0}^T, y_{t_c=0}^T, d_{t_c=0}^T, (y_{t_c}^{SP})^T, u_{t_c=-1}^T, Y_{t_c}^T]^T$$
$$\forall\ t_c \in \{0, 1, ..., N_c\} \tag{18}$$

Table 3. Tuning Parameters for the mpMPC of the CSTR for Example 1

mpMPC design parameters	value
N_c	6
M_c	2
QR	$\begin{bmatrix} 10^2 & 0 & 0 \\ 0 & 10 & 0 \\ 0 & 0 & 10 \end{bmatrix}$
$R1$	50
$P1$	90
$y_{\min}$	$[0, 0, 0]^T$
$y_{\max}$	$[1, 1, 1]^T$
$u_{\min}$	$[0, 0, 0]^T$
$u_{\max}$	$[1, 1, 1]^T$
$d_{\min}$	0
$d_{\max}$	500

where the additional term ε_{t_c} is the slack variables, $P1$ is the penalty matrix, $Pur_{\min}$ is the minimum purity level required to trigger accumulation in the storage tanks, y_{*,t_c} is the concentration of the product of interest at time t_c, and $\mathcal{M}$ is a big-M parameter. The binary switch parameter Y_{t_c} determined by an upper level decision maker dictates the product of interest, and binary switch variable z_{t_c} determines the optimal input subspace. The soft constraints are constructed on y_{*,t_c} via slack variables ε_{t_c} to minimize the transition time by penalizing any production below the threshold purity level throughout the output horizon. Therefore, the non-negative slack variables ε_{t_c} contribute to the objective function if and only if the purity of the product of interest is below the threshold. Note that any process disturbances, such as reactant concentrations at the feed stream, can be easily incorporated in the control scheme without modifying the overall framework by simply introducing them as additional parameters.

The optimization problem given in eq 18 is reformulated as a mpMIQP problem and solved via the POP toolbox to generate the map of optimal control actions as affine functions of the system parameters. (The complete solution of the problem along with the approximate model can be downloaded from http://paroc.tamu.edu.) The explicit expression of the control action is designed to (i) track a set point determined by an upper level decision maker, (ii) adapt proactively to changing operating modes (i.e., shifting between different products), and (iii) minimize the transition time by penalizing impure production periods.

Note that the mpMPC formulation utilizes a single state space model with piecewise affine inputs that are selected via binary switch variables, z_{t_c}. Therefore, the control scheme single-handedly recognizes the dynamics of the transitions between the production periods. Although the stability of the system under such transitions is left outside the scope of this study, it can be further investigated following the approach proposed by Grieder et al.[56]

Closed-Loop Validation. The control scheme is validated by exhaustive testing against the high-fidelity dynamic model under various scheduling decisions. Figure 5 presents a 2 h closed-loop operation with two distinct operational modes. The process starts from zero product concentration and goes through a shift from the production of P_3 to production of P_2 at t = 60 min. This shift is manually enforced by changing the

DOI: 10.1021/acs.iecr.7b04457
Ind. Eng. Chem. Res. 2018, 57, 3963−3976

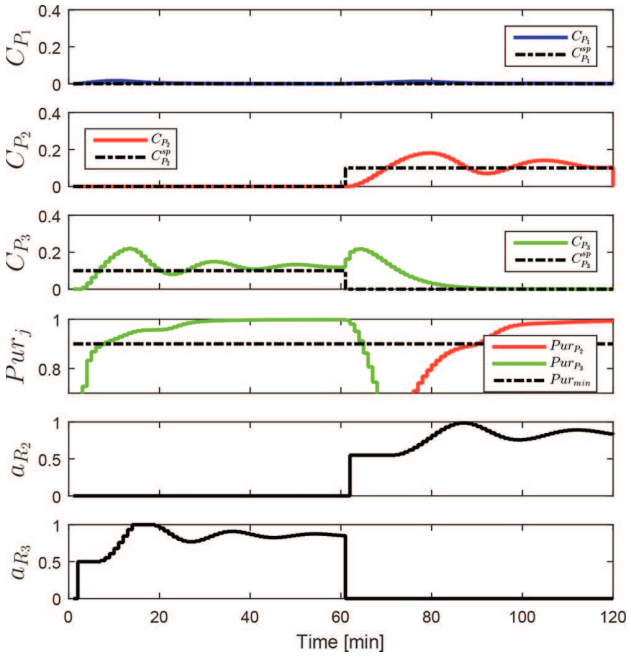

Figure 5. Closed-loop validation of the mpMPC against the high-fidelity model for Example 1.

concentration set points from $y^{SP} = [0, 0, 0.1]^T$ to $y^{SP} = [0,0.1,0]^T$.

The closed-loop simulation in Figure 5 validates the mpMPC as it (i) tracks the set points of three product concentrations, (ii) handles operations at different production modes, (iii) prioritizes purity satisfaction to minimize transition time, and (iv) maintains feasible operation by keeping the system within specified bounds. Note that the entirety of the closed loop simulations uses only one mpMPC scheme in both the production and the transition periods. Therefore, the controller parameters are tuned regarding every possible transition between the products.

High-Fidelity Model with the mpMPC Embedded. The initial high-fidelity model given in eqs 10−15 is integrated with the derived control scheme in the form of eq 5.

Model Approximation. To keep the example tangible, only the mole balance around the storage tanks is considered in the upper level schedule, while the dynamics of the CSTR is accounted for in the lower level surrogate model formulation. The bilinear $Q_{\text{total}}C_{P_j}$ term in eq 13 results into a nonconvex mpMINLP problem, for which only approximate solution algorithms exist. Hence, we postulate a mpMILP problem, for which POP toolbox features an exact algorithm, via replacing eq 13 with eq 19.

$$\frac{dW_{P_j}}{dt} = F_{P_j} - DR_{P_j} \tag{19}$$

where F_{P_j} is the molar product flow rate at the exit of the CSTR. Having merely linear terms in eq 19 enables the formulation of a mpMILP in the subsequent step.

The lower level surrogate model, on the other hand, is identified via MATLAB System Identification Toolbox as described in the previous section. Three surrogate models are derived for three distinct operational modes (provided in the Supporting Information with their respective step and impulse responses).

Design of the Scheduler and the Surrogate Model. The scheduler for this problem is designed to minimize the inventory cost, while satisfying continuous demand rates for the three products forecasted through the scheduling horizon.

$$\begin{aligned}
\min_{F_{j,t_s}, Y_{P_j,t_s}} \quad & J(\theta) = \sum_{j=1}^{} \sum_{t_s=1}^{N_s} \alpha_{P_j}^T W_{t_s} \\
\text{s.t.} \quad & W_{P_j,t_s+1} = W_{P_j,t_s} + \Delta t_s F_{j,t_s} - \Delta t_s DR_{P_j,t_s} \\
& \sum_{j=1} F_{j,t_s} = F_{\text{total},t_s} \\
& \sum_{j=1} Y_{P_j,t_s} = 1 \\
& F_{\min} Y_{P_j,t_s} \le F_{j,t_s} \le F_{\max} Y_{P_j,t_s} \\
& W_{\min} \le W_{P_j,t_s} \le W_{\max} \\
& DR_{\min} \le DR_{P_j,t_s} \le DR_{\max} \\
& \theta = [W_{P_j,t_s=0}, DR_{P_j,t_s}]^T \\
& Y_{P_j,t_s} \in \{0, 1\}, \forall\, t_s \in \{0, 1, ..., N_s\}
\end{aligned} \tag{20}$$

where Y_{P_j,t_s} denotes the selected product P_j to be manufactured at time t_s, F_{j,t_s} is the molar product flow rate, Δt_s is the sampling time for the schedule. Note that eq 19 is discretized into time steps Δt_s.

The system parameters for eq 20 are given in Table 4.

Table 4. System Parameters for the Scheduler of the CSTR for Example 1

system parameters	value
N_s	3
α[$/h.mol]	$[1.0, 1.5, 1.8]^T$
Δt_s [min]	60
$F_{\min}$	$[0, 0, 0]^T$
$F_{\max}$	$[50, 50, 50]^T$
$W_{\min}$	$[0, 0, 0]^T$
$W_{\max}$	$[50, 50, 50]^T$
$D_{\min}$	$[0, 0, 0]^T$
$D_{\max}$	$[60, 60, 60]^T$

The bridge between the mpMPC and the scheduler derived in eqs 18 and 20 is constructed based on eq 8. Analogous to the mpMPC, the surrogate model also features the soft constraints to enforce a threshold purity level.

$$\begin{aligned}
\min_{Q_{\text{total},t_{sm}}, C^{SP}_{P_j,t_{sm}}, \varepsilon'_{t_{sm}}} J(\theta) = & \sum_{t_{sm}=0}^{M_{sm}} (Q_{\text{total},t_{sm}} - \tilde{Q}_{\text{total},t_{sm}})^T R' \\
& \times (Q_{\text{total},t_{sm}} - \tilde{Q}_{\text{total},t_{sm}}) + \sum_{t_{sm}=1}^{N_{sm}} \varepsilon'^T_{t_{sm}} P1' \varepsilon'_{t_{sm}}
\end{aligned}$$

DOI: 10.1021/acs.iecr.7b04457
Ind. Eng. Chem. Res. 2018, 57, 3963−3976

Table 5. System Parameters for the Surrogate Model of the CSTR for Example 1

system parameters	model 1	model 2	model 3
N_{sm}	10	10	10
M_{sm}	1	1	1
T_{sm} [min]	6	6	6
R'	10^3	$\begin{bmatrix} 10^{-4} & 0 \\ 0 & 10^{-1} \end{bmatrix}$	$\begin{bmatrix} 10^{-4} & 0 \\ 0 & 10^{-1} \end{bmatrix}$
$P1'$	10^4	10^6	10^8
$y_{\min}$ [mol/L]	$[0, 0, 0]^T$	$[0, 0, 0]^T$	$[0,0,0]^T$
$y_{\max}$ [mol/L]	$[1, 1, 1]^T$	$[1, 1, 1]^T$	$[1, 1, 1]^T$
$Q_{\min}$ [L/min]	0	0	0
$Q_{\max}$ [L/min]	500	500	500
$C^{SP}_{\min}$ [mol/L]	$[0, 0, 0]^T$	$[0, 0, 0]^T$	$[0, 0, 0]^T$
$C^{SP}_{\max}$ [mol/L]	$[1, 1, 1]^T$	$[1, 1, 1]^T$	$[1, 1, 1]^T$

s.t. eqs S1−S3 (Supporting Information)

$$\tilde{Q}_{\text{total},t_{sm}} = \frac{F_{\text{total},t_{sm}}}{C_{P_s,t_{sm}=0}}$$

$$y_{\min} \le y_{t_{sm}} \le y_{\max}$$

$$Q_{\min} \le Q_{\text{total},t_{sm}} \le Q_{\max}$$

$$C^{SP}_{\min} \le C^{SP}_{P_j,t_{sm}} \le C^{SP}_{\max}$$

$$-y_{*,t_{sm}} + Pur_{\min} \sum_i y_{i,t_{sm}} \le -\varepsilon'_{t_{sm}}$$

$$0 \le \varepsilon'_{t_{sm}} \le 1$$

$$\theta = \left[x^T_{t_{sm}}, \frac{F_{\text{total},t_{sm}}}{C_{P_s,t_{sm}=0}} \right]^T$$

$$\forall\, t_{sm} \in \{0, 1, ..., N_{sm}\} \qquad (21)$$

Note that the formulation given in eq 21 is only valid for the product of interest. Hence, three separate formulations are constructed for each product. Tuning of the surrogate model parameters is based on heuristic decisions that yield a desirable performance in the closed loop validation, and the parameters are given in Table 5.(The complete solution of the problem along with the approximate model can be downloaded from http://paroc.tamu.edu.)

Closed-Loop Validation of the Overall Scheme. Closing the loop of the CSTR is performed via testing the scheduling and control scheme against the high fidelity model. Figure 6 presents a 12 h operation with the scheduler, the surrogate model, and the controller operating in tandem with the dynamic model while no specific knowledge of the demand profile is assumed. (The explicit expressions of the simultaneous decisions at t = 60 min and t = 105 min are demonstrated in the Supporting Information.) The scheduler (i) maintains low inventory levels and (ii) adapts to the changes in the demand profile, while satisfying the continuous demand rate. Because of the rolling horizon strategy, the schedule is updated at every discretization step T_s, with the current inventory level and the new demand profile N_s time steps into the future. Note that the resultant production sequence is different from a cyclic schedule reported in Flores-Tlacuahuac and Grossmann[7] and Zhuge and Ierapetritou,[29] since the demand rates in this work are time variant.

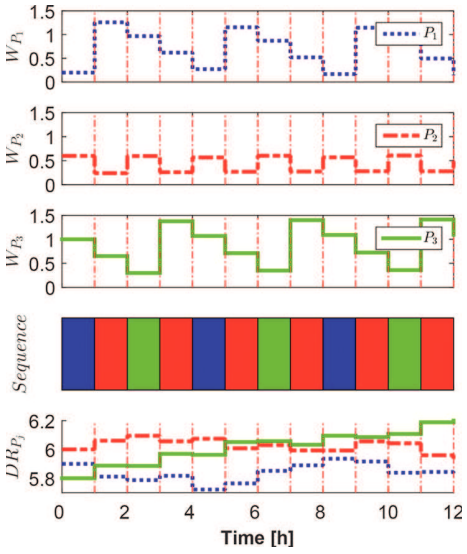

Figure 6. Closed-loop validation of the scheduling scheme for Example 1.

Figure 7 presents a snapshot of the first 6 h of operation, focusing on the lower level surrogate model decisions. The

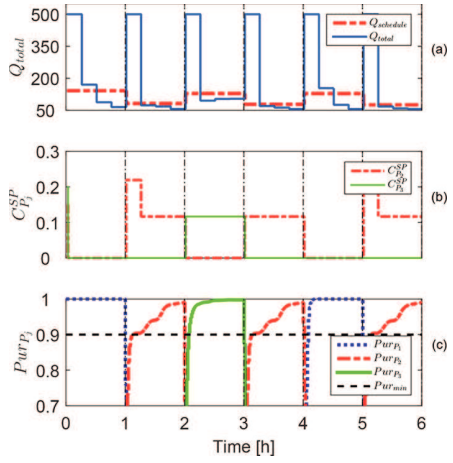

Figure 7. Closed-loop simulation of the CSTR for the first 6 h of operation for Example 1: (a) volumetric flow rate determined by the scheduler, and the corrected action of the surrogate model; (b) product concentration set points; (c) product purities.

volumetric feed flow rate from the schedule and the surrogate model are juxtaposed in Figure 7a to emphasize the corrective actions of the latter. During the transition between production regimes, the surrogate model saturates Q_{total} at its upper bound to purge the previous product left in the reactor. The transitions can also be monitored from the product purities presented in Figure 7c. The surrogate model and the mpMPC operate in tandem to drive the system above the threshold purity level. The transitions to product P_2 specifically show that the integrated schedule and control scheme prioritizes the purity satisfaction to minimize the transition time.

Note the following:

- The explicit expressions for the optimal scheduling decisions enable rescheduling with a small computational

DOI: 10.1021/acs.iecr.7b04457
Ind. Eng. Chem. Res. 2018, 57, 3963−3976

cost when disruptive events occur in the product demands.

- The transition time is not determined explicitly by the integrated scheduling and control scheme, but is minimized through soft constraints in the surrogate model and controller formulations. The non-negative slack variables ε_{t_c} and $\varepsilon'_{t_{sm}}$ in eqs 18 and 21 are nonzero only if the product concentration of interest is below the threshold level, and contribute to the objective function $J(\theta)$ proportional to $P1$ and $P1'$, respectively. A more accurate approach would be allocating every time step for all products with binary variables to determine whether the purity threshold is satisfied. However, employing such a large number of binary variables in a multiparametric programming problem results in an exponential increase in the computational burden. Hence, we alleviate this problem via the soft constraint formulation.
- The heavy penalty terms for purity satisfaction in the surrogate models result in steep changes in Q_{total} during the transitions, as observed in Figure 7. The upper level schedule is unable to make such corrective decisions due to its large time step. The lower level surrogate model provides time varying targets and set points for the controller due to the embedded closed loop dynamics in its formulation.
- Because of the strong nonlinearity of the high-fidelity model, the input space is partitioned as presented in eq 17. Finer partitions will yield more accurate controllers at the expense of increased computation time to generate the offline maps of optimal actions.
- Utilizing the maps of optimal solutions for the control, surrogate model, and schedule actions eases the online implementation. Calculation of the optimal actions is reduced from an online optimization problem to a simple look-up table algorithm and evaluation of an affine function.

3.2. Example 2 – Two CSTRs Operating in Parallel.

Problem Definition. This case study extends the CSTR example from section 3.1 to encompass two identical CSTRs operating in parallel. Because of the identical design of the reactors, the mpMPC and the surrogate model driving the closed-loop system are identical as well. Hence, the derivation of their formulations and attaining the explicit maps of solutions are omitted.

Cooperative operation of independent reactors requires a centralized scheduling scheme to allocate the production tasks on different reactors. However, the identical nature of the two closed-loop system dynamics creates a multiplicity of solutions, as the reactors are indistinguishable to the upper level schedule. Hence, the scheduling formulation presented in eq 20 is modified to (i) account for the previous production regime as an additional uncertain parameter and (ii) penalize transitions between consecutive production regimes to break multiple solutions. Inclusion of the retrospective information provides a distinction between the reactors, eliminating any redundant transitions between the products. The mathematical representation of the described modification is provided in eq 22.

$$\Gamma_s = \sum_{t_s=0}^{N_s} \psi |Y_{P_j,t_s} - Y_{P_j,t_s-1}| \tag{22}$$

where ψ is a very small number that virtually penalizes the changes in the operational mode. Equation 22 can be reformulated as follows to maintain the linear structure of the scheduling problem.

$$\Gamma_s = \sum_{t_s=0}^{N_s} \psi^T \overline{Y}_{t_s}$$

s.t.

$$Y_{P_j,t_s} - Y_{P_j,t_s-1} \le \overline{Y}_{t_s}$$

$$-Y_{P_j,t_s} + Y_{P_j,t_s-1} \le \overline{Y}_{t_s}$$

$$0 \le \overline{Y}_{t_s} \le 1 \tag{23}$$

where $\overline{Y}_{t_s}$ is an auxiliary variable.

Design of the Scheduler. The scheduling formulation presented in eq 20 is extended to account for multiple production lines, and modified with eq 23 to eliminate multiple solutions.

$$\min_{F_{j,t_s,l}, Y_{P_j,t_s,l}, \overline{Y}_{t_s,l}} J(\theta) = \sum_{j=1}^{N_s} \sum_{t_s=1}^{N_s} \alpha_{P_j}^T W_{P_j,t_s} + \sum_{l=1}^{N_{\text{CSTR}}} \sum_{t_s=0}^{N_s} \psi^T \overline{Y}_{t_s,l}$$

s.t. $$W_{P_j,t_s+1} = W_{P_j,t_s} + \sum_{l=1}^{N_{\text{CSTR}}} \Delta t_s F_{j,t_s,l} - \Delta t_s DR_{P_j,t_s}$$

$$\sum_{j=1} F_{j,t_s,l} = F_{\text{total},t_s,l}$$

$$\sum_{j=1} Y_{P_j,t_s,l} = 1$$

$$Y_{P_j,t_s,l} - Y_{P_j,t_s-1,l} \le \overline{Y}_{t_s,l}$$

$$-Y_{P_j,t_s,l} + Y_{P_j,t_s-1,l} \le \overline{Y}_{t_s,l}$$

$$0 \le \overline{Y}_{t_s,l} \le 1$$

$$F_{\min} Y_{P_j,t_s,l} \le F_{j,t_s,l} \le F_{\max} Y_{P_j,t_s,l}$$

$$W_{\min} \le W_{P_j,t_s} \le W_{\max}$$

$$DR_{\min} \le DR_{P_j,t_s} \le DR_{\max}$$

$$\theta = [W_{P_j,t_s=0},\ DR_{P_j,t_s},\ Y_{P_j,t_s=-1,l}]^T$$

$$Y_{P_j,t_s,l} \in \{0, 1\},\ \forall\ t_s \in \{0, 1, ..., N_s\},$$
$$\forall\ l \in \{1, 2, ..., N_{\text{CSTR}}\} \tag{24}$$

where the additional weight ψ is tuned to be 0.001, and the number of the CSTRs, N_{CSTR}, is 2 by the problem definition.

Closed-Loop Validation. The validation of the overall scheduling and control scheme is presented in Figure 8. The scheduler, the surrogate model, and the controller are operated in tandem with the high fidelity model for 12 h under a randomized demand profile. The integrated scheduling and control scheme delivers the additional task to coordinate multiple reactors to operate in parallel while satisfying the continuous demand rate. The inclusion of eq 23 in the objective function breaks the symmetry between the reactors and coordinates the production sequence. Consequently,

DOI: 10.1021/acs.iecr.7b04457
Ind. Eng. Chem. Res. 2018, 57, 3963−3976

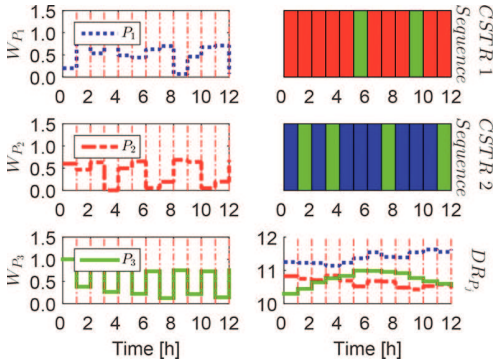

Figure 8. Closed-loop validation of the integrated scheduling and control scheme on two CSTRs for Example 2.

uninterrupted manufacturing of the product of interest is maintained without redundant shifts between the reactors.

Figure 9 presents the evolution of the schedule with time for the first 4 h of operation. Note that the demand scenario is

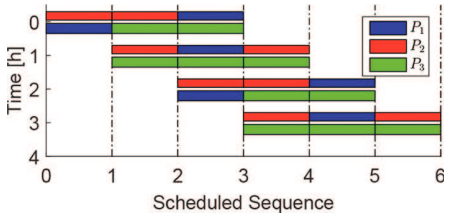

Figure 9. Realization of the schedule with time for Example 2. Top bars and bottom bars represent CSTR 1 and CSTR 2, respectively.

updated every hour in a rolling horizon manner, allowing rescheduling of the production sequence and the target quantities by utilizing the offline maps of optimal scheduling actions.

4. CONCLUSIONS

We have presented a systematic framework to integrate process scheduling and control in continuous systems via multiparametric programming. We have derived optimal scheduling and control actions simultaneously based on a single high fidelity model. We take advantage of the synergistic interactions between the two decision making mechanisms to yield offline maps of optimal operations as explicit affine expressions at both long and short terms of a process. The generic structure of the framework renders it suitable for a software prototype toward enterprise-wide optimization.

This work aims to increase the operability, flexibility, and profitability of process systems through improving the scheduling and control decisions. Nevertheless, the processes with comparable capital and operating costs necessitate the consideration of the design aspect simultaneously with the scheduling and control. Hence, our current effort focuses on the unification of these three multiscale problems.

■ ASSOCIATED CONTENT

Supporting Information

The Supporting Information is available free of charge on the ACS Publications website at DOI: 10.1021/acs.iecr.7b04457.

The state space matrices of the surrogate models, the step and impulse responses of the open and closed loop systems, and an instance of the simultaneous decisions (PDF)

■ AUTHOR INFORMATION

Corresponding Author

*E-mail: stratos@tamu.edu.

ORCID

Baris Burnak: 0000-0001-6118-8711

Efstratios N. Pistikopoulos: 0000-0001-6220-818X

Notes

The authors declare no competing financial interest.

■ ACKNOWLEDGMENTS

Financial support from the National Science Foundation (Grant No. 1705423), Texas A&M Energy Institute, and EPSRC (EP/M027856/1) is greatly acknowledged.

■ NOMENCLATURE

Lowercase Letters

a = Molar fraction
b = Constant term of the critical region boundary
d = Measured disturbance
e = Plant-model mismatch
f = First principle equation
g = First principle equation
h = Optimal control action expression
k = Rate constant ($L/mol.min$)
m = Optimal scheduling action expression
r = Constant term in the explicit control law
t = Time (min)
tr = Transition variable
u = Control action
x = State of the system
y = Output of the system
z = Binary decision at the control level

Uppercase Letters

$\mathcal{R}$ = Reaction rate (mol/L·min)
C = Concentration (mol/L)
CR = Critical region
DR = Demand rate (mol/min)
F = Molar flow rate (mol/min)
J = Objective value
K = Linear term of the explicit control law
L = Linear term of the critical region boundary
M = Control horizon
N = Output horizon
NC = Number of critical regions
P = Objective function
P = Product
P = Terminal weight matrix
$P1$ = Penalty matrix for the slack variables
Pur = Purity
Q = Volumetric flow rate (L/min)
Q = Weight matrix of the states
QR = Weight matrix of the outputs
R = Reactant
R = Weight matrix of the manipulated variables
$R1$ = Weight matrix for the changes in the manipulated variables
S = Continuous scheduling variables

DOI: 10.1021/acs.iecr.7b04457
Ind. Eng. Chem. Res. 2018, 57, 3963−3976

Sc = Degrees of freedom of the system avaiable to the schedule
V = Reactor volume (L)
W = Inventory level (mol)
Y = Binary scheduling variables

Greek Letters

α = Operational cost parameter
β = Transition cost parameter
ϕ = Cost parameter for the manipulated variable
τ = Time
Θ = Closed and bounded set
θ = Parameter
ε = Slack variable

Subscripts

c = Control
i = Reactant index
j = Product index
k = Discretized time step
n = Critical region index
s = Schedule
sm = Surrogate model

Superscripts

f = Feed stream
q = Linear model index
SP = Set point

Accents

$'$ = Surrogate level counterpart
$-$ = Auxiliary variable
$\wedge$ = Predicted
$\sim$ = Scheduling level counterpart

REFERENCES

(1) Grossmann, I. Enterprise-wide optimization: A new frontier in process systems engineering. *AIChE J.* **2005**, *51*, 1846−1857.
(2) Floudas, C. A.; Niziolek, A. M.; Onel, O.; Matthews, L. R. Multi-scale systems engineering for energy and the environment: Challenges and opportunities. *AIChE J.* **2016**, *62*, 602−623.
(3) Pistikopoulos, E. N.; Diangelakis, N. A. Towards the integration of process design, control and scheduling: Are we getting closer? *Comput. Chem. Eng.* **2016**, *91*, 85−92.
(4) Engell, S.; Harjunkoski, I. Optimal operation: Scheduling, advanced control and their integration. *Comput. Chem. Eng.* **2012**, *47*, 121−133.
(5) Baldea, M.; Harjunkoski, I. Integrated production scheduling and process control: A systematic review. *Comput. Chem. Eng.* **2014**, *71*, 377−390.
(6) Du, J.; Park, J.; Harjunkoski, I.; Baldea, M. A time scale-bridging approach for integrating production scheduling and process control. *Comput. Chem. Eng.* **2015**, *79*, 59−69.
(7) Flores-Tlacuahuac, A.; Grossmann, I. E. Simultaneous cyclic scheduling and control of a multiproduct CSTR. *Ind. Eng. Chem. Res.* **2006**, *45*, 6698−6712.
(8) Harjunkoski, I.; Nyström, R.; Horch, A. Integration of scheduling and control-Theory or practice? *Comput. Chem. Eng.* **2009**, *33*, 1909−1918.
(9) Flores-Tlacuahuac, A.; Grossmann, I. An effective MIDO approach for the simultaneous cyclic scheduling and control of polymer grade transition operations. *Comput.-Aided Chem. Eng.* **2006**, *21*, 1221−1226.
(10) Terrazas-Moreno, S.; Flores-Tlacuahuac, A.; Grossmann, I. E. Simultaneous cyclic scheduling and optimal control of polymerization reactors. *AIChE J.* **2007**, *53*, 2301−2315.
(11) Flores-Tlacuahuac, A.; Grossmann, I. E. Simultaneous Cyclic Scheduling and Control of Tubular Reactors: Single Production Lines. *Ind. Eng. Chem. Res.* **2010**, *49*, 11453−11463.
(12) Flores-Tlacuahuac, A.; Grossmann, I. E. Simultaneous cyclic scheduling and control of tubular reactors: Parallel production lines. *Ind. Eng. Chem. Res.* **2011**, *50*, 8086−8096.
(13) Gutiérrez-Limón, M. A.; Flores-Tlacuahuac, A.; Grossmann, I. E. A Multiobjective Optimization Approach for the Simultaneous Single Line Scheduling and Control of CSTRs. *Ind. Eng. Chem. Res.* **2012**, *51*, 5881−5890.
(14) Gutiérrez-Limón, M. A.; Flores-Tlacuahuac, A.; Grossmann, I. E. MINLP formulation for simultaneous planning, scheduling, and control of short-period single-unit processing systems. *Ind. Eng. Chem. Res.* **2014**, *53*, 14679−14694.
(15) Mitra, K.; Gudi, R. D.; Patwardhan, S. C.; Sardar, G. Resiliency issues in integration of scheduling and control. *Ind. Eng. Chem. Res.* **2010**, *49*, 222−235.
(16) Nie, Y.; Biegler, L. T.; Wassick, J. M. Integrated Scheduling and Dynamic Optimization of Batch Processes Using State Equipment Networks. *AIChE J.* **2012**, *58*, 3416−3432.
(17) Nie, Y.; Biegler, L. T.; Villa, C. M.; Wassick, J. M. Discrete time formulation for the integration of scheduling and dynamic optimization. *Ind. Eng. Chem. Res.* **2015**, *54*, 4303−4315.
(18) Chu, Y.; You, F. Integration of production scheduling and dynamic optimization for multi-product CSTRs: Generalized Benders decomposition coupled with global mixed-integer fractional programming. *Comput. Chem. Eng.* **2013**, *58*, 315−333.
(19) Chatzidoukas, C.; Perkins, J. D.; Pistikopoulos, E. N.; Kiparissides, C. *Chem. Eng. Sci.* **2003**, *58*, 3643−3658.
(20) Chatzidoukas, C.; Kiparissides, C.; Perkins, J. D.; Pistikopoulos, E. N. Optimal grade transition campaign scheduling in a gas-phase polyolefin FBR using mixed integer dynamic optimization. *Comput.-Aided Chem. Eng.* **2003**, *15*, 744−747.
(21) Chu, Y.; You, F. Integration of scheduling and control with online closed-loop implementation: Fast computational strategy and large-scale global optimization algorithm. *Comput. Chem. Eng.* **2012**, *47*, 248−268.
(22) Mahadevan, R.; Doyle, F. J., III; Allcock, A. C. Control-Relevant Scheduling of Polymer Grade Transitions. *AIChE J.* **2002**, *48*, 1754−1764.
(23) Capón-García, E.; Guillén-Gosálbez, G.; Espuña, A. Integrating process dynamics within batch process scheduling via mixed-integer dynamic optimization. *Chem. Eng. Sci.* **2013**, *102*, 139−150.
(24) Park, J.; Du, J.; Harjunkoski, I.; Baldea, M. Integration of scheduling and control using internal coupling models. *Comput.-Aided Chem. Eng.* **2014**, *33*, 529−534.
(25) Bhatia, T.; Biegler, L. Dynamic optimization in the design and scheduling of multiproduct batch plants. *Ind. Eng. Chem. Res.* **1996**, *5885*, 2234−2246.
(26) Allgor, R.; Barton, P. Mixed-integer dynamic optimization I: problem formulation. *Comput. Chem. Eng.* **1999**, *23*, 567−584.
(27) Nyström, R. H.; Franke, R.; Harjunkoski, I.; Kroll, A. *Comput. Chem. Eng.* **2005**, *29*, 2163−2179.
(28) Prata, A.; Oldenburg, J.; Kroll, A.; Marquardt, W. Integrated scheduling and dynamic optimization of grade transitions for a continuous polymerization reactor. *Comput. Chem. Eng.* **2008**, *32*, 463−476.
(29) Zhuge, J.; Ierapetritou, M. G. Integration of scheduling and control with closed loop implementation. *Ind. Eng. Chem. Res.* **2012**, *51*, 8550−8565.
(30) Huercio, A.; Espuña, A.; Puigjaner, L. Incorporating on-line scheduling strategies in integrated batch production control. *Comput. Chem. Eng.* **1995**, *19*, 609−614.
(31) Kopanos, G. M.; Georgiadis, M. C.; Pistikopoulos, E. N. Energy production planning of a network of micro combined heat and power generators. *Appl. Energy* **2013**, *102*, 1522−1534.
(32) Kopanos, G. M.; Pistikopoulos, E. N. Reactive scheduling by a multiparametric programming rolling horizon framework: A case of a network of combined heat and power units. *Ind. Eng. Chem. Res.* **2014**, *53*, 4366−4386.

DOI: 10.1021/acs.iecr.7b04457
Ind. Eng. Chem. Res. 2018, 57, 3963−3976

(33) Subramanian, K.; Maravelias, C. T.; Rawlings, J. B. A state-space model for chemical production scheduling. *Comput. Chem. Eng.* **2012**, *47*, 97−110.
(34) Subramanian, K.; Rawlings, J. B.; Maravelias, C. T.; Flores-Cerrillo, J.; Megan, L. Integration of control theory and scheduling methods for supply chain management. *Comput. Chem. Eng.* **2013**, *51*, 4−20.
(35) Würth, L.; Hannemann, R.; Marquardt, W. A two-layer architecture for economically optimal process control and operation. *J. Process Control* **2011**, *21*, 311−321.
(36) Diangelakis, N. A.; Burnak, B.; Pistikopoulos, E. N. A multi-parametric programming approach for the simultaneous process scheduling and control—Application to a domestic cogeneration unit. Foundations of Computer Aided Process Operations/Chemical Process Control. Tucson, Arizona, January 8−122017.
(37) Diangelakis, N. A.; Pistikopoulos, E. N. Model-based multi-parametric programming strategies towards the integration of design, control and operational optimization. *27th European Symposium on Computer-Aided Process Engineering*; (ESCAPE-27) Elsevier, 2017; pp 1867−1872.
(38) Dias, L. S.; Ierapetritou, M. G. Integration of scheduling and control under uncertainties: Review and challenges. *Chem. Eng. Res. Des.* **2016**, *116*, 98−113.
(39) Honkomp, S. J.; Mockus, L.; Reklaitis, G. V. A framework for schedule evaluation with processing uncertainty. *Comput. Chem. Eng.* **1999**, *23*, 595−609.
(40) Lin, X.; Janak, S. L.; Floudas, C. A. A new robust optimization approach for scheduling under uncertainty: I. Bounded uncertainty. *Comput. Chem. Eng.* **2004**, *28*, 1069−1085.
(41) Janak, S. L.; Lin, X.; Floudas, C. A. A new robust optimization approach for scheduling under uncertainty. II. Uncertainty with known probability distribution. *Comput. Chem. Eng.* **2007**, *31*, 171−195.
(42) Patil, B. P.; Maia, E.; Ricardez-sandoval, L. A. *Integration of Scheduling, Design, and Control of Multiproduct Chemical Processes Under Uncertainty*; Wiley, 2015, *61*.
(43) Koller, R. W.; Ricardez-Sandoval, L. A. A Dynamic Optimization Framework for Integration of Design, Control and Scheduling of Multi-product Chemical Processes under Disturbance and Uncertainty. *Comput. Chem. Eng.* **2017**, *106*, 147−159.
(44) Chu, Y.; You, F. Model-based integration of control and operations: Overview, challenges, advances, and opportunities. *Comput. Chem. Eng.* **2015**, *83*, 2−20.
(45) Bassett, M.; Dave, P.; Doyle, F.; Kudva, G.; Pekny, J.; Reklaitis, G.; Subrahmanyam, S.; Miller, D.; Zentner, M. Perspectives on model based integration of process operations. *Comput. Chem. Eng.* **1996**, *20*, 821−844.
(46) Floudas, C. A.; Lin, X. Continuous-time versus discrete-time approaches for scheduling of chemical processes: A review. *Comput. Chem. Eng.* **2004**, *28*, 2109−2129.
(47) Baldea, M.; Du, J.; Park, J.; Harjunkoski, I. Integrated Production Scheduling and Model Predictive Control of Continuous Processes. *AIChE J.* **2015**, *61*, 4179−4190.
(48) Pistikopoulos, E. N.; Diangelakis, N. A.; Oberdieck, R.; Papathanasiou, M. M.; Nascu, I.; Sun, M. PAROC - An integrated framework and software platform for the optimization and advanced model-based control of process systems. *Chem. Eng. Sci.* **2015**, *136*, 115−138.
(49) Bansal, V.; Sakizlis, V.; Ross, R.; Perkins, J. D.; Pistikopoulos, E. N. New algorithms for mixed-integer dynamic optimization. *Comput. Chem. Eng.* **2003**, *27*, 647−668.
(50) Diangelakis, N. A.; Burnak, B.; Katz, J.; Pistikopoulos, E. N. Process Design and Control Optimization: A Simultaneous Approach by Multi-Parametric Programming. *AIChE J.* **2017**, *63*, 4827−4846.
(51) Bemporad, A.; Morari, M.; Dua, V.; Pistikopoulos, E. N. The explicit linear quadratic regulator for constrained systems. *Automatica* **2002**, *38*, 3−20.
(52) Löfberg, J. YALMIP: A toolbox for modeling and optimization in MATLAB. *Proceedings of the IEEE International Symposium on Computer-Aided Control System Design* **2004**, 284−289.
(53) Oberdieck, R.; Diangelakis, N. A.; Papathanasiou, M. M.; Nascu, I.; Pistikopoulos, E. N. POP - Parametric Optimization Toolbox. *Ind. Eng. Chem. Res.* **2016**, *55*, 8979−8991.
(54) Diangelakis, N. A. Model-based multi-parametric programming strategies towards the integration of design, control and operational optimization. Ph.D. Thesis, Imperial College London, London, United Kingdom, 2017.
(55) Oberdieck, R.; Diangelakis, N. A.; Avraamidou, S.; Pistikopoulos, E. N. On unbounded and binary parameters in multi-parametric programming: applications to mixed-integer bilevel optimization and duality theory. *J. Glob. Optim.* **2017**, *69*, 587.
(56) Grieder, P.; Kvasnica, M.; Baotic, M.; Morari, M. Low Complexity Control of Piecewise Affine Systems with Stability Guarantee. *Proceedings of the 2004 American Control Conference, Boston, Massachusetts* **2004**, 1196−1201.

DOI: 10.1021/acs.iecr.7b04457
Ind. Eng. Chem. Res. 2018, 57, 3963−3976